 doi:10.20944/preprints202210.0372.v1

Article

Study of the Carbochlorination Process with $CaCl_2$ and Water Leaching for the Extraction of Li, Co, and Ni From Spent Lithium-Ion Batteries

Yarivith C. González [1,2,*], Lorena Alcaraz [3,*], Francisco J. Alguacil [3], Lucía Barbosa [1,2], Jorge González [1,2], and Félix A. López[3]

[1] Instituto de Investigación en Tecnología Química (INTEQUI-CONICET), A. Brown 1455, San Luis, D5700, Argentina; yarithgon11@gmail.com; lucia.ib100@gmail.com; jgonza@unsl.edu.ar
[2] Facultad de Química Bioquímica y Farmacia (FQBF), UNSL, Ejército de los Andes 950, San Luis, D5700, Argentina; yarithgon11@gmail.com; lucia.ib100@gmail.com; jgonza@unsl.edu.ar
[3] Centro Nacional de Investigaciones Metalúrgicas (CENIM), Consejo Superior de Investigaciones Científicas (CSIC). Avda. Gregorio del Amo, 8. 28040, Madrid, España; alcaraz@cenim.csic.es; fjalgua@cenim.csic.es; f.lopez@csic.es
* Correspondence: alcaraz@cenim.csic.es (Tel.: +34-911992202); yarithgon11@gmail.com

Abstract: The abundant use of lithium-ion batteries (LIBs) in a wide variety of electric devices and vehicles will generate a large number of depleted batteries, which contain several valuable metals such as Li, Co, Mn, and Ni present in the structure of the cathode material ($LiMO_2$). The present work investigates chemical, technological, and environmental aspects in the treatment of such wastes, development of a methodology for the extraction of lithium, cobalt, nickel, manganese, and graphite by a carbochlorination pyrometallurgical process. Mixtures of cathode and anode materials (called black mass, mixed oxides of Li, Co, Ni, Mn, and graphite) from different LIBs, carbon black (as reducing agent), and $CaCl_2$ (as chlorinating agent) were used. Non-isothermal thermogravimetric tests up to 850°C and isothermal tests at 700°C of the mixtures in an inert atmosphere were carried out. It was experimentally observed that the $LiMO_2$-C-$CaCl_2$ reaction takes place at 700°C. LiCl, Ni, and Co were obtained as final products, and to a lesser extent, CoO, NiO, and MnO_2. $CaCO_3$ was also obtained as a by-product. The obtained results show that carbochlorination is an efficient and effective alternative route for the extraction and recovery of metals from different LIBs, focused on the sustainability and circular economy

Keywords carbochlorination; spent lithium-ion batteries; circular economy; recycle; LiCl

1. Introduction

Lithium-ion batteries (LIBs) are widely used in portable devices due to their high energy density to weight ratio, reduced memory effect, and a significant number of charge/discharge cycles [1]. In addition, LIBs are being increasingly used in electromobility technologies for transportation and the alternative energy industry [2,3]. Thus, the global lithium market is expected to increase by around 87% by 2025 due to the anticipated expansion of LIBs for their large applications. The increase in demand for LIBs causes some concern about the supply of the primary resources needed to manufacture new batteries in the medium term [4]. Thus, they recycle is of the utmost interest.

In general, LIBs consist of a cathode, an anode, and a polymeric separator impregnated with an electrolyte that enables the ionic conduction of the lithium ions. The active material used in the cathode can vary depending on the manufacturer [3]. The most common compounds of the cathode material are $LiCoO_2$, $LiMn_2O_4$, and $LiFePO_4$, among others [5]. On the other hand, the active material commonly used in the anode is graphite [6,7].

Because of the limited lifetime of LIBs, 11 million tons of spent batteries are estimated to be produced by 2030 [7,8]. Recently, a report by the United Nations University revealed

 doi:10.20944/preprints202210.0372.v1

that a high percentage of electronic waste including spent LIBs is highly polluting because they contain i.e. Li, Co, Mn, and Ni among others. It is predicted that 80 GWh of LIBs will be discarded as waste by 2025 [9]. This figure is equivalent to the global battery market of 2017, which corresponds to 64,000 tons of Li and 18,000 tons of Co. Therefore, proper management of the final disposal of spent LIBs is of great concern.

Recycling spent batteries is an interesting alternative to deal with both the supply issues to manufacture new batteries and the polluting effects of discarded batteries [10]. The recycling of discarded LIBs focuses mainly on the recovery of strategic metals: lithium and transition metals such as nickel, manganese, and cobalt. These recovered metals could be reused in the manufacture of new battery electrodes [11,12]. Also, the recovered lithium could be used in many other applications, including glass and ceramics, lubricants and greases, aluminum production, and air treatment. Even in the medical field, lithium is applied in various treatments: bipolar disorder, depression, dental, and headaches [13]. The recovery of cobalt and nickel from spent LIBs could also be beneficial because the extraction of these metals from primary resources is expensive and highly polluting. The main reserves are found in the Democratic Republic of Congo. Much of the extraction work is done by hand, posing a risk to the environment and human health [14]. Therefore, recycling spent batteries may contribute to the circular economy [15–17].

Many studies have been conducted focusing on the recovery of metals from spent LIBs by applying different methods. Hydrometallurgy and pyrometallurgy are the most typical methods [18–20]. Hydrometallurgy uses different leaching agents including hydrochloric acid (HCl), nitric acid (HNO_3), and phosphoric acid (H_3PO_4) to extract the targeted metals. Whereas, pyrometallurgy uses heat to induce a chemical change in the components of the LIBs to extract the metals of interest [19].

Carbothermic reduction has become an important pyrometallurgical method [21–23]. This method implies the use of a carbonaceous material fulfilling the function of a reducing agent. The metals are directly recovered as Li_2CO_3, CoO, and MnO. Temperatures as low as 550°C were found to be optimum for metal recovery using carbon black (CB) as the reducing agent [18]. Chlorination roasting was also studied as an alternative pyrometallurgical method to recover metals such as LiCl, $CoCl_2$, $MnCl_2$, and $NiCl_2$ [24,25]. An extraction yield as high as 100% was reached at 900°C and 90 min using chlorine as chlorinating agent [26]. The main key to these processes is to break the chemical bonds of the cathode material with the general formula $LiMO_2$ (usually M = Co or Ni). Thus, Li and M can be converted into two different species that can be separated by precipitation, phase separation, solvent extraction, or in the form of oxides according to the applied method [1]. Then, we propose an innovative carbochlorination process as an alternative method to recover metals from spent LIBs by combining the important aspects of carbothermal reduction and chlorination roasting [18,26].

Carbochlorination consists of the chlorination reaction leading to metallic chlorides in presence of a chlorinating agent and a carbonaceous material in a dry atmosphere [27]. It is favored over direct chlorination regarding thermodynamic and kinetic aspects which in turn results in an important reduction of the reaction temperature. The carbonaceous material fulfills a dual function: as an oxygen acceptor favoring metal reduction and as a catalyst generating and capturing active chlorine species [28–30]. Regarding the chlorinating agent, various compounds including gaseous chlorine (Cl_2), HCl, CCl_4, $MgCl_2$, and $CaCl_2$ were used depending on the metal or sample to be chlorinated [31]. Calcium chloride ($CaCl_2$) is a very low-cost reagent and can be acquired as a by-product of the Solvay process. This chloride has already been used to extract lithium as lithium chloride from β-spodumene [25].

In the present work, a carbochlorination method using $CaCl_2$ as chlorinating agent and carbon black (CB) as a reducing agent was researched to recover metals from spent LIBs. Different experimental conditions were evaluated to establish an efficient process.

Preprints (www.preprints.org) | NOT PEER-REVIEWED | Posted: 25 October 2022 doi:10.20944/preprints202210.0372.v1

2. Materials and Methods

The starting materials were three samples called black mass samples (BM). The source of one BM was smartphones, and the source of the other two BM was electric/hybrid vehicles. The BM from smartphones were called SBM and those from electric/hybrid vehicles were called VBM-1 and VBM-2. $CaCl_2$) at 99% purity (Panreac Applichem) was used as the chlorinating agent. In addition, commercial CB was used as a reducing agent. Subsequently, a mixture was made with each BM in 50:20:30% w/w proportions of BM, $CaCl_2$, and CB using a mortar. The proportions of $CaCl_2$ and CB were calculated based on the percentage of lithium present in the BM. All carbochlorination experiments were carried out in a nitrogen atmosphere of 99.99% v/v.

2.1. Equipment

The structural characterization of the starting black masses and the products obtained after the reaction were made by X-ray diffraction (XRD). With the exception of subsequently called soluble products (SP) solids, XRD measurements were collected on a Rigaku D-Max-IIIC diffractometer operated at 30 kV and 20 mA, using the Kα radiation of Cr and filter of V. The structural characterization of the initial and final materials was evaluated by X-ray diffraction (XRD) using an PANalytical Multi-Purpose diffractometer model X'Pert PRO MPD, which is equipped with a high-temperature chamber for use with temperature diffraction measurements with a Cu anode (Cu Kα radiation). The XRD measurements at 70 ºC were done using a heating ramp of 10 ºC min^{-1}.

Metal concentrations in aqueous solutions were analyzed by Atomic Absorption Spectroscopy (AAS) using a Perkin Elmer 1100B spectrophotometer. Previously, each BM was dissolved with aqua regia solution and moderate heating for several hours. Then, the final solution was filtered, and the obtained insoluble solid was dried to calculate the graphite carbon content in each sample. The determination of the percentage of carbon in the initial samples was carried out using the combustion technique in an induction furnace and infrared absorption detection.

The morphology of all the samples was analyzed by field emission scanning electron microscopy (FE-SEM) using a LEO 1450VP microscope, equipped with an EDAX Genesis 2000 energy dispersive spectrometer, and a Hitachi S-4800 equipped with an energy-dispersive X-ray microanalyzer (EDX). For SEM observations, the powder samples were placed on an adhesive conductive carbon disk. In the case of the NS-samples, the powders were embedded into a conductive resin due to the magnetism of the products.

The non-isothermal calcination tests were done in a thermogravimetric system suitable for working in corrosive and non-corrosive atmospheres designed in our laboratory [32]. Isothermal carbochlorination tests were carried out in a high alumina tubular reactor, with a circulating-flow system. The sample was contained in a high alumina crucible that was then placed inside the reactor at the required temperature and for the specific working time.

3. Experimental procedure

3.1. Non-isothermal experiments

The BM/$CaCl_2$ and BM/$CaCl_2$/CB mixtures were analyzed by thermogravimetric analysis (TGA). The mixture samples were studied by thermogravimetric analysis (TGA). 250 mg of each sample were put in a large alumina crucible. The crucible containing the sample was placed inside a tubular reactor. Immediately, the heating program of 5 °C/min was run until reached 850°C. A nitrogen current circulated at 20 mL min^{-1} during the whole heating period. After the experiment, the sample was cooled down and withdrawn from the reactor for further analysis.

3.2. Isothermal experiments

Both BM/$CaCl_2$ and BM/$CaCl_2$/carbon black mixtures were heated at isothermal conditions. Temperatures of 350 °C, 500 °C, and 700 °C were investigated, using a different

Preprints (www.preprints.org) | NOT PEER-REVIEWED | Posted: 25 October 2022 doi:10.20944/preprints202210.0372.v1

sample for each temperature. These temperatures were selected by analyzing the derivative of the TGA curve of the BM/$CaCl_2$ and BM/$CaCl_2$/carbon black mixtures. The sample was put in a large alumina crucible that was then placed inside the tubular reactor, with a through-flow system circulating 20 mL·min^{-1} of nitrogen. The heating program was run at 5 ° C·min^{-1} until reach the working temperature and then the temperature was held constant for 60 min. After the reaction time is fulfilled, the crucible containing the calcined sample was removed from the reactor and cooled. The variation in mass after calcination was recorded in Table 2. Subsequently, the calcined sample was washed with distilled water at 70 ° C. After washing, the slurry obtained was filtered. The filtrate solution was analyzed by AAS to measure lithium concentration. Then, the filtrate solution and the wet solid retained on the filter were left in an oven until drying. The crystallized solid from the filtrate was identified as soluble products (SP) and the dried solid as non-soluble products (NSP). SP and NSP samples were characterized by DRX and SEM-EDS.

Lithium extraction was calculated using equation (1):

$$x = \frac{m_f}{m_i} \cdot 100 \qquad (1)$$

where X is the lithium extraction in percentage, m_i is the initial mass of Li in the cathode material sample, determined using the concentration of Li in the original black mass sample, and m_f is the mass of Li in the soluble products, determined using the concentration of Li in the filtrate solution obtained after washing the calcined samples.

4. Results and discussion

4.1. Characterization of the initial black mass samples

After the leaching of the BM with aqua regia, a black solid remained insoluble. This residue could be graphite, proceeding from the anode material. Table 1 showed metal and carbon concentrations measured by AAS and combustion, respectively. The calculated carbon content was around 30-33 % for the three samples.

Table 1. Elemental composition of the black mass samples (weight percentage %).

Sample	Li	Co	Mn	Ni	Cu	C
SBM 1	4.5	30	4.30	0.90	0.30	33.3
VBM-1	3.11	5.62	10.1	11.2	2.2	32
VBM-2	5.2	3.2	n.d	41.2	1.2	30.9

n.d. = not detected

The XRD patterns for SBM, VBM-1, and VBM-2 are shown in Figure 1. Diffraction maxima were found that can be attributed to the phases of $LiCoO_2$ for SBM, $LiNi_{0.5}Mn_{1.5}O_4$ for VM-1, and a lesser extent $LiNiO_2$ for VM-2. Several reflection maxima corresponding to the carbon graphite phase were detected in the three samples SBM, VBM-1, and VBM-2. Thus, the high carbon content in black mass samples is related to crystalline carbon graphite. This result agrees well with the chemical composition of the initial samples. Figure 2 shows SEM micrographs and EDS spectra from particles of each black mass sample. VBM-1 and VBM-2 samples are made up of agglomerates of rounded primary particles. The micrograph of the SBM sample exhibits particles without a regular form having a smooth surface and sharp edges. Regarding EDS results, the element detected are as follows: C, O, Ni, Al, Mn, and Co in VBM-1; C, O, Al, Co, and Ni in VBM-2, and C, O, and Co, and Si in SBM

Preprints (www.preprints.org) | NOT PEER-REVIEWED | Posted: 25 October 2022 doi:10.20944/preprints202210.0372.v1

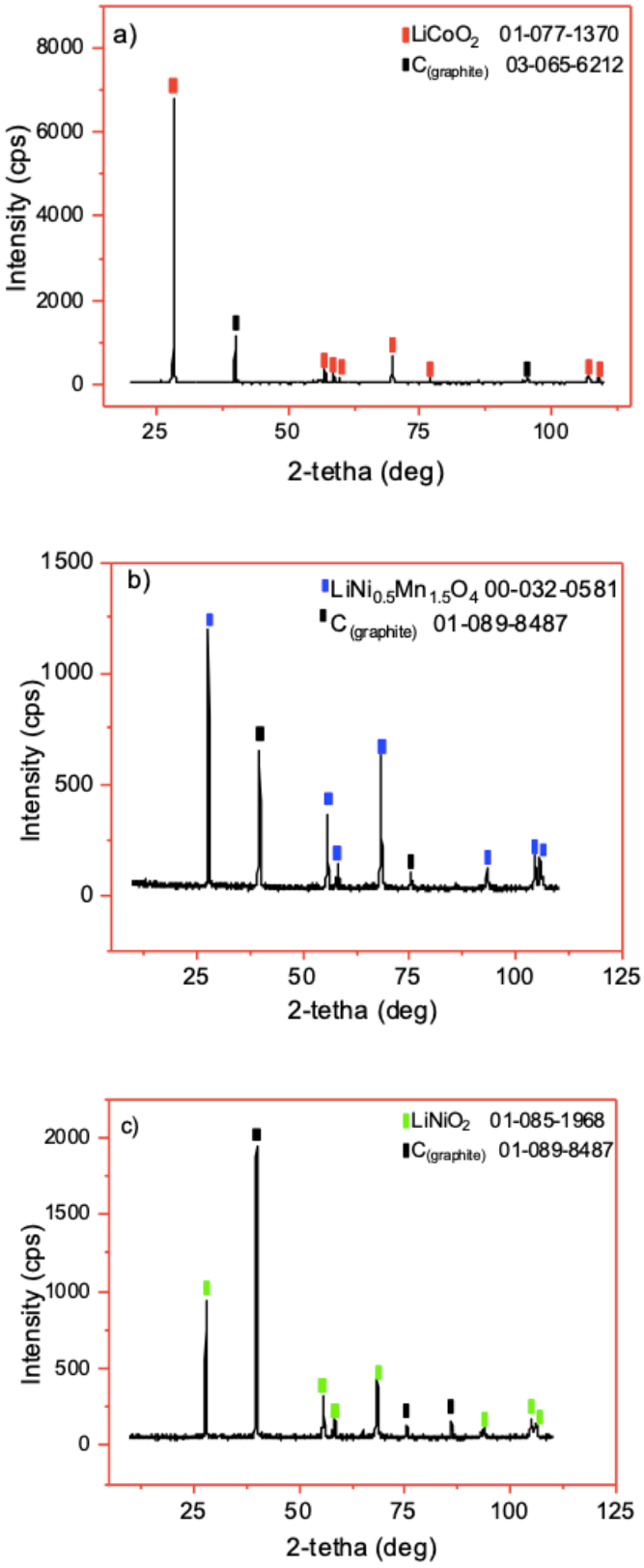

Figure 1. Diffractograms of the black mass samples from spent LIBs: a) SBM, b) VBM-1 and c) VBM-2.

Preprints (www.preprints.org) | NOT PEER-REVIEWED | Posted: 25 October 2022 doi:10.20944/preprints202210.0372.v1

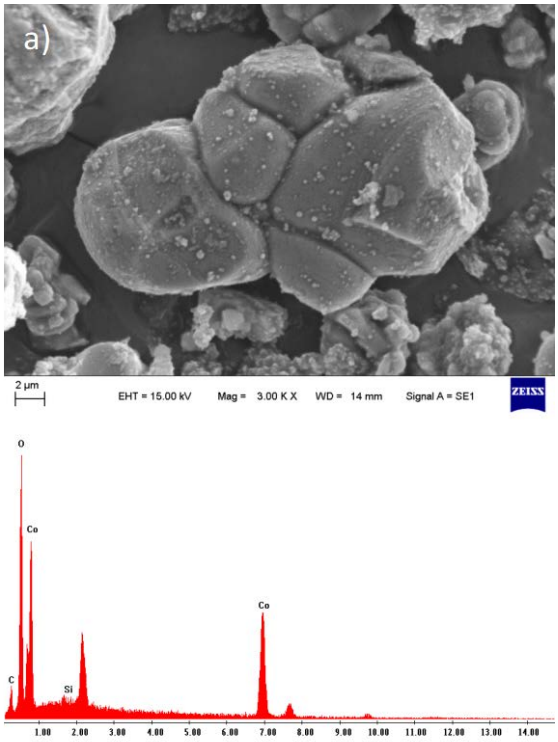

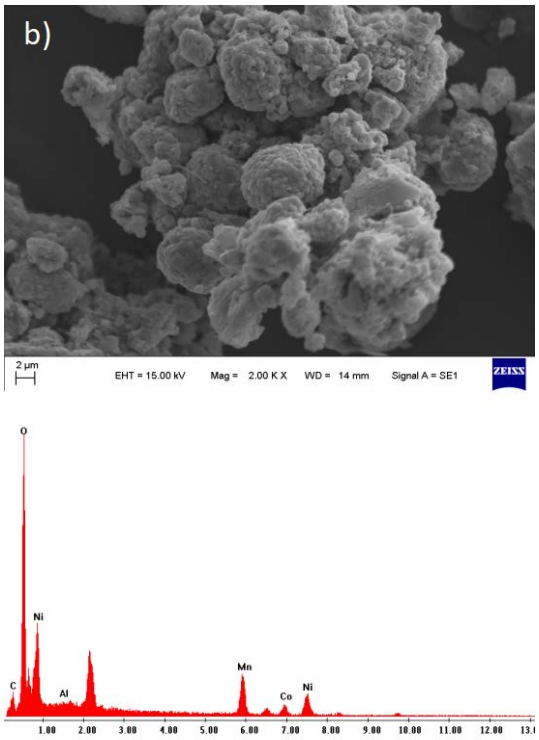

Preprints (www.preprints.org) | NOT PEER-REVIEWED | Posted: 25 October 2022 doi:10.20944/preprints202210.0372.v1

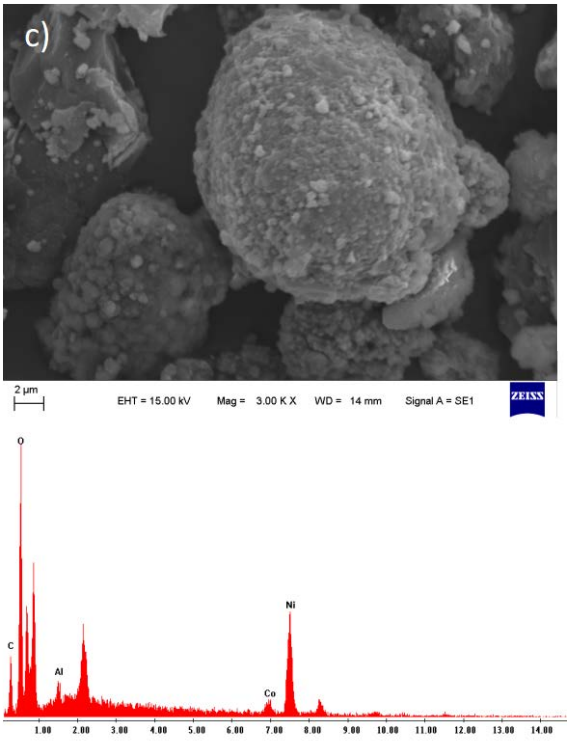

Figure 2. SEM micrographs and EDS spectra from particles of each black mass sample, a) SBM, b) VBM-1, and c) VBM-2.

4.2. Non-isothermal experiments

Figure 3 shows the thermograms obtained after the non-isothermal experiment. The first mass loss can be distinguished between 40 and 210 °C, which can be associated with loss of moisture for all samples. Between 212 and 695 °C a small mass loss of approximately 3%, 7%, and 8% for SBM, VBM-1, and VBM-2, respectively, is observed this loss of mass is attributed to the loss of wetting and possible impurities (agglutinate) of the mixture. Between 700 and 850 °C, a marked mass loss zone is detected: 20%, 24%, and 32% for SBM, VBM-1, and VBM-2, respectively. This last mass loss could be related to the release of CO_2 as a product of the reduction of cobalt, nickel, and manganese and the release of CO_2. It is expected that during the heat treatment lithium chloride is produced. Thus, the mass loss detected between 700 and 800 °C could also be attributed in part to either the volatilization of volatile lithium chloride or the reaction of lithium chloride with the crucible made up of alumina [33].

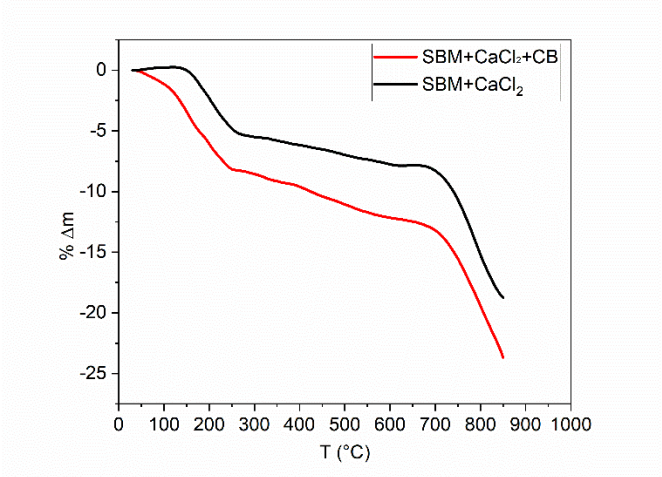

Preprints (www.preprints.org) | NOT PEER-REVIEWED | Posted: 25 October 2022 doi:10.20944/preprints202210.0372.v1

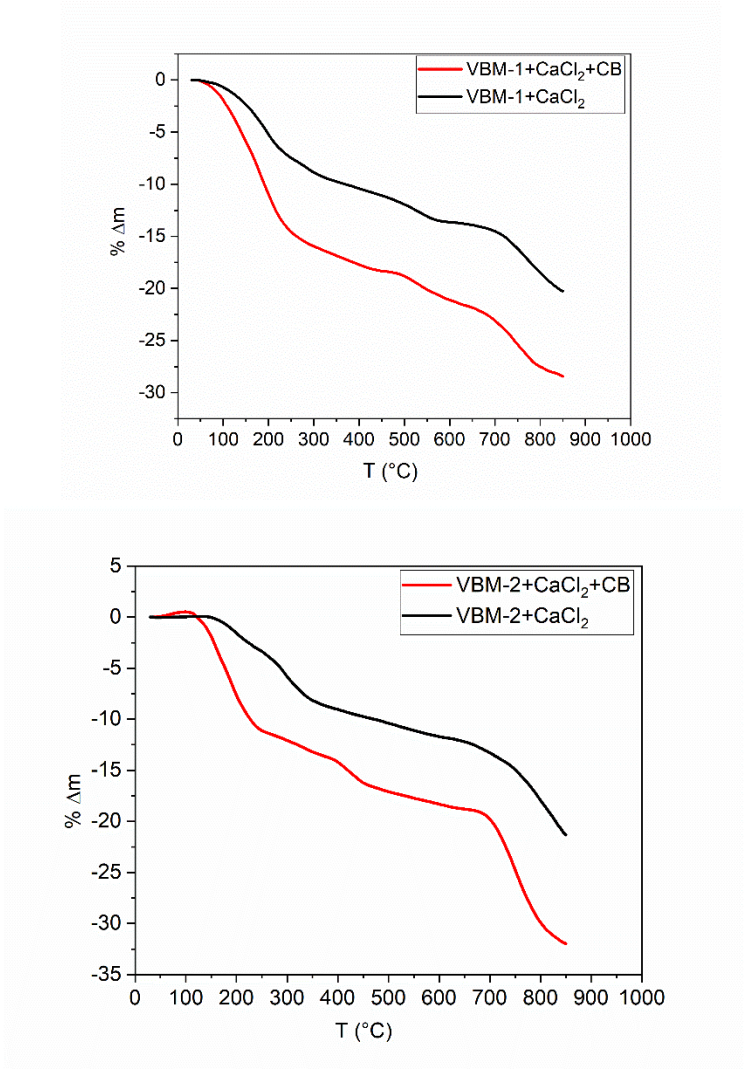

Figure 3. TGA of the BM/$CaCl_2$ and BM/$CaCl_2$/carbon black mixture in N_2 stream.

4.3. Isothermal experiments

Table 2 shows the mass variation of BM/$CaCl_2$ and BM/$CaCl_2$/carbon black mixtures after being heat-treated at isothermal conditions. These mass losses coincide with those shown in figure 3, being associated with the loss of impurity in the sample, at 500 degrees the increase in mass loss is associated with the release of CO_2 by the carbon effect, and finally at 700 degrees with the reduction of Ni and Co to the metallic state.

Table 2. Mass loss of the mixtures calcined at isothermal conditions.

Temperature (ºC)	BM/$CaCl_2$	Δm(%)	BM/$CaCl_2$/carbon black	Δm(%)
350	VBM-1	7	VBM-1	24
	VBM-2	12	VBM-2	20
	SBM	4	SBM	27
500	VBM-1	10	VBM-1	27
	VBM-2	14	VBM-2	25
	SBM	6	SBM	27
700	VBM-1	12	VBM-1	30
	VBM-2	15	VBM-2	30
	SBM	7	SBM	31

 doi:10.20944/preprints202210.0372.v1

Figure 4 shows the XRD patterns of NSP samples, obtained after each isothermal calcination of both mixtures BM/$CaCl_2$ and BM/$CaCl_2$/CB. Figures 4a, 4b, and 4c show the results of VBM-1, VBM-2, and SBM, respectively. Regarding VBM-1, at 350 °C, the peaks of the $LiNi_{0.5}Mn_{1.5}O_4$ phase find in the original sample are still present in the XRD pattern of the NSP sample. At 500 °C, the peak intensity of the $LiMn_{0.5}Ni_{1.5}O_2$ phase decreases significantly but the decrease is more noticeable in the case of the VBM-1/$CaCl_2$/CB system. We can infer that at 500 °C, $LiMn_{0.5}Ni_{1.5}O_2$ starts to react with $CaCl_2$, and the reaction is favored when CB is present, since peaks of $CaCO_3$ and mixed Ni and Mn oxide start to be noticeable. At 700 °C, the $LiMn_{0.5}Ni_{1.5}O_2$ is no longer detected in either case. In the case of the VBM-1/$CaCl_2$ system, peaks characteristic of mixed Ni and Mn oxide and $CaCO_3$ are predominantly observed. In the case of the VBM-1/$CaCl_2$/CB system, very intense peaks corresponding to metallic Ni can be observed. Peaks of $CaCO_3$ and MnO_2 are also identified as reaction products.

With respect to VBM-2, at 350 °C, the peaks of $LiNiO_2$ phase found in the original sample are also identified in the NP sample for both systems VBM-2/$CaCl_2$ and VBM-2/$CaCl_2$/CB. At 500 °C, the peak intensities of the $LiNiO_2$ phase decreased drastically for the VBM-2/$CaCl_2$. In the case of the VBM-2/$CaCl_2$/CB system, the phase $LiNiO_2$ is no longer detected, instead, NiO and $CaCO_3$ are detected as reaction products. Therefore, we can infer that at 500 °C, $LiNiO_2$ starts to react with $CaCl_2$. When the temperature is increased to 700 °C, NiO and $CaCO_3$ are the reaction products for the VBM-2/$CaCl_2$ system. Whereas, metallic Ni, $CaCO_3$, and NiO are identified as reaction products for the VBM-2/$CaCl_2$/CB system. The peaks of the NiO phase are largely reduced in intensity.

Concerning SBM, at 350 °C, the $LiCoO_2$ phase originally found in the cathode material is still present in the XRD pattern of the NSP sample for both systems SBM/$CaCl_2$ and SBM/$CaCl_2$/CB. In the case of the SBM/$CaCl_2$ system, at 500 °C, the peak intensities of the $LiCoO_2$ phase significantly decrease, the characteristic peaks of the CoO phase start to be noticeable and only one peak corresponding to the $CaCO_3$ phase can be detected. In the case of the SBM/$CaCl_2$/CB system, the characteristic peaks of the $LiCoO_2$ phase disappear completely, whereas the peaks of the CoO and $CaCO_3$ phases are well-defined. Regarding the SBM/$CaCl_2$ system, at 700 °C, the identified crystalline products are CoO and $CaCO_3$. For the SBM/$CaCl_2$/CB system, in addition to CoO and $CaCO_3$, characteristic peaks of metallic Co are also identified, indicating a superior reducing effect of the CB.

The graphite phase originally found in the black mass samples was also identified in all NSP samples. The comparative analysis of the XRD patterns of the NSP samples indicates that the original oxide present in the black mass sample is completely attacked at 700 °C for both studied systems.

Preprints (www.preprints.org) | NOT PEER-REVIEWED | Posted: 25 October 2022 doi:10.20944/preprints202210.0372.v1

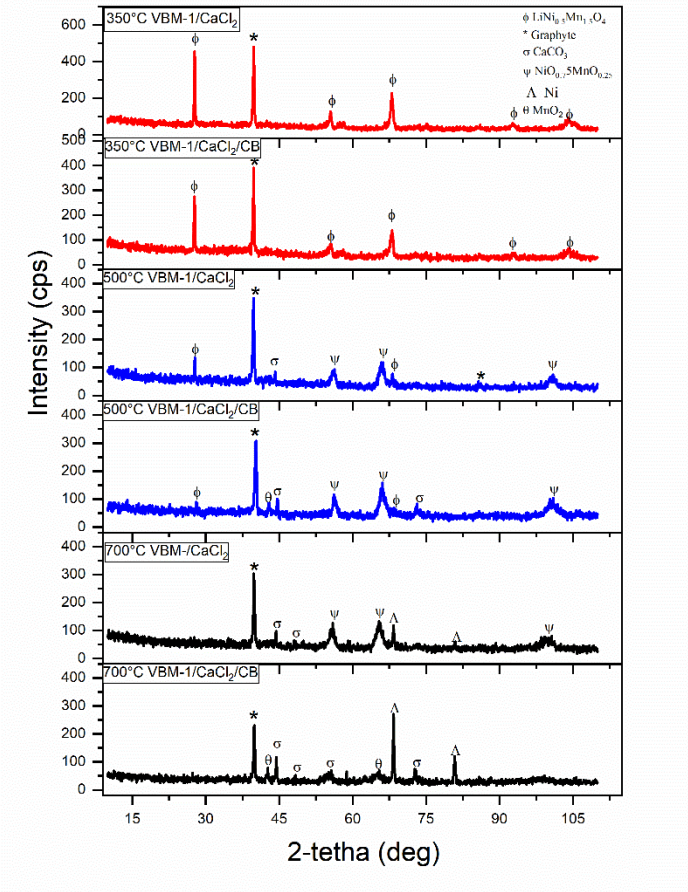

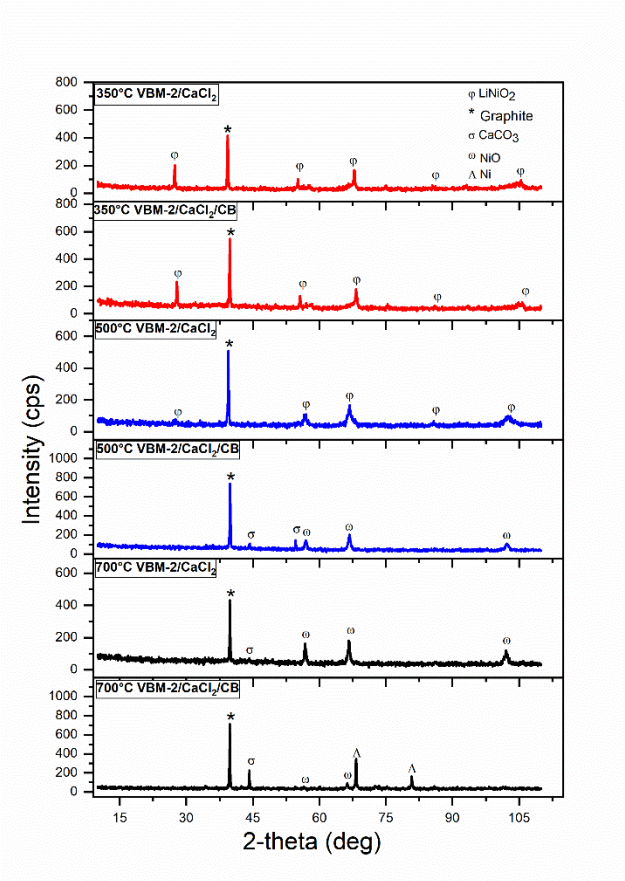

Preprints (www.preprints.org) | NOT PEER-REVIEWED | Posted: 25 October 2022 doi:10.20944/preprints202210.0372.v1

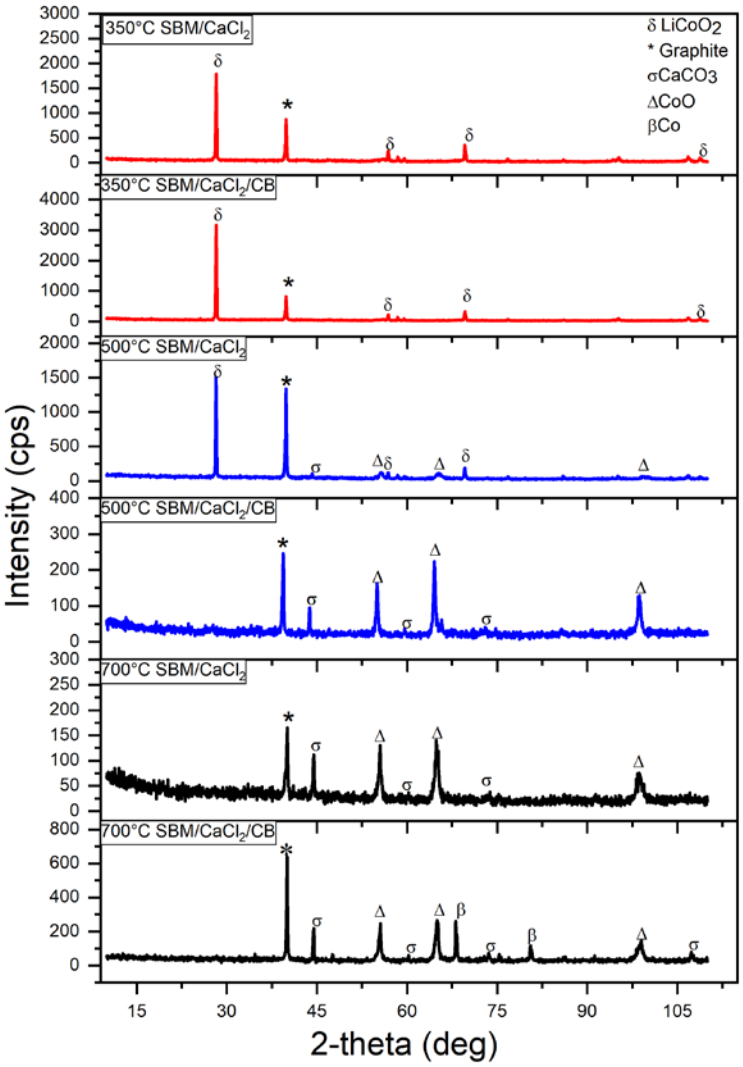

Figure 4. XRD patterns of the NSP samples obtained after the isothermal calcination of both mixtures BM/$CaCl_2$ and BM/$CaCl_2$/CB a) VBM-1 b) VBm-2 and c) SBM.

Figure 5 exhibits the SEM micrographs and EDS spectra of NSP samples from the calcination of the BM/$CaCl_2$/CB sample at 700 °C. If we draw a comparison with the SEM micrographs from Figure 2 indicated that, after the thermal treatment, the samples are attacked because they have very different morphology after the heat treatment. Regarding EDS results, the element detected are as follows: C, O, Ni, Al, Ca, Mn, and Co in VBM-1; C, O, Ni, Al, Ca, and Co in VBM-2, and C, O, Ca, Mn, Co, and Ni in SBM. Considering the XRD results, the detection of Ca by EDS in the three NSP samples can be associated with the $CaCO_3$ phase.

In the case of VBM-1, the presence of C can be associated with the graphite phase detected by XRD. The presence of Ni can be associated with metallic Ni, while the presence of Mn with the MnO_2 phase. The presence of Al is due to the Al impurity identified in the original black mass sample. The presence of Co cannot be associated with any crystalline phase since Co-containing phases are not detected in the XRD pattern of the corresponding NSP sample.

Regarding VBM-2, the presence of C can also be associated with the graphite phase detected by XRD. The presence of Ni can be associated with the NiO phase and metallic

Preprints (www.preprints.org) | NOT PEER-REVIEWED | Posted: 25 October 2022 doi:10.20944/preprints202210.0372.v1

Ni. The presence of Al is also due to the Al impurity detected in the original black mass sample. The presence of Co cannot be associated with any crystalline phase since Co-containing phases are not detected in the XRD pattern of the corresponding NSP sample.

With respect to SBM, the presence of C can be associated with the graphite phase detected by XRD. The presence of Co can be associated with the CoO phase and metallic Co. Neither the presence of Ni nor Mn can be associated with any crystalline phases since Co- and Mn-containing phases are not detected in the XRD pattern of the corresponding NSP sample. Ni and Mn from the original sample are detected by AAS.

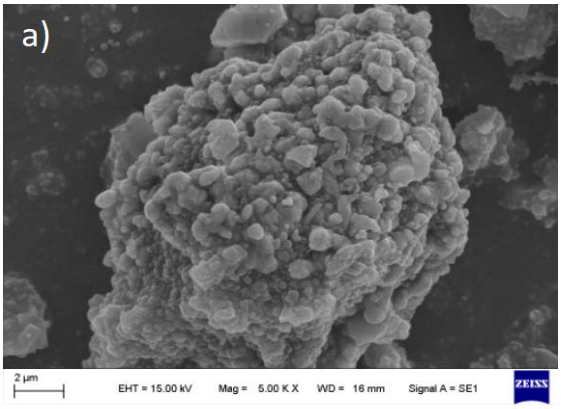

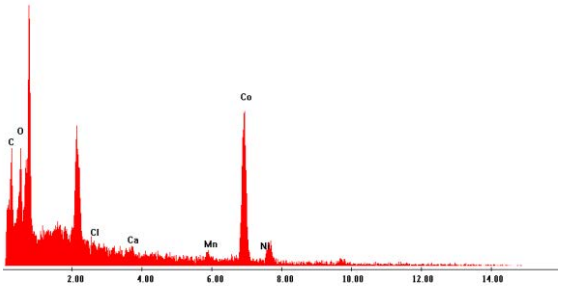

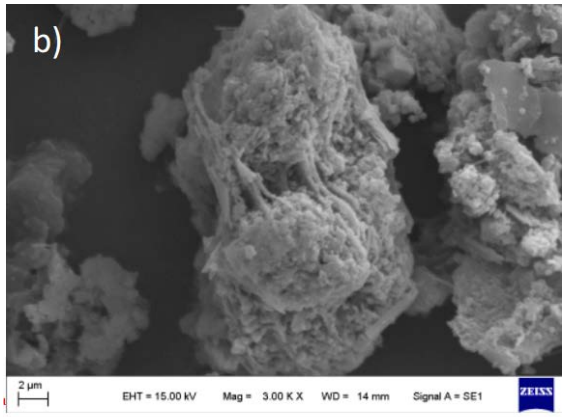

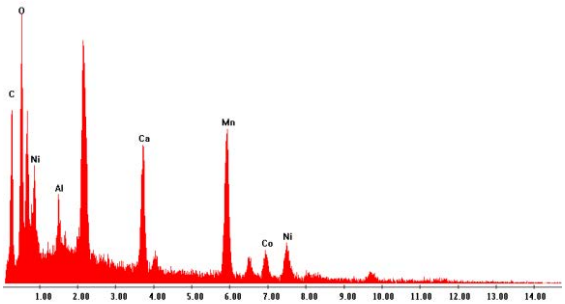

Preprints (www.preprints.org) | NOT PEER-REVIEWED | Posted: 25 October 2022 doi:10.20944/preprints202210.0372.v1

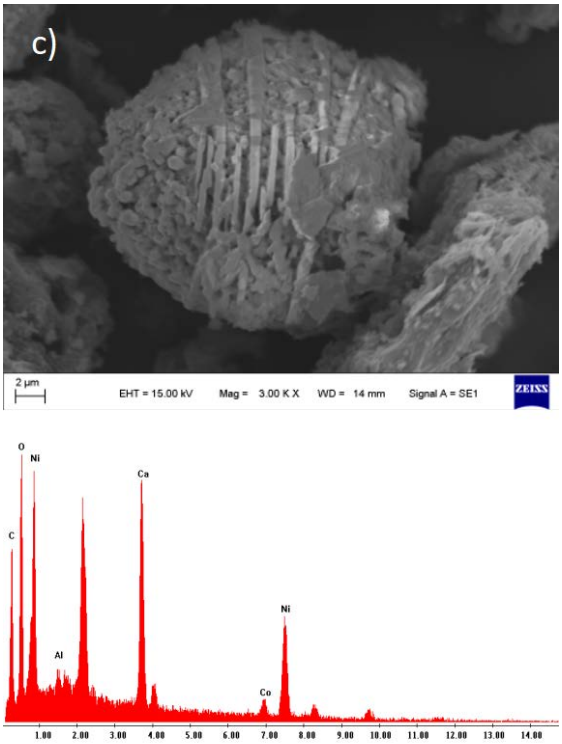

Figure 5. SEM micrographs and EDS spectra of NSP samples from the calcination of BM/$CaCl_2$/CB at 700°C. a) SBM, b) VBM-1 and c) VBM-2.

Figure 6 shows the XRD patterns of the SP samples, obtained after the isothermal experiment performed at 700 °C for the BM/$CaCl_2$/CB system. Figures 4a, 4b, and 4c show the results of SBM, VBM-1, and VBM-2, respectively. All patterns exhibit characteristic diffraction maxima of LiCl and hydrated LiCl. Minor characteristic peaks of LiF were also detected; this result can be attributed to possible impurities associated with traces of electrolyte that may have still been present in the original black mass sample.

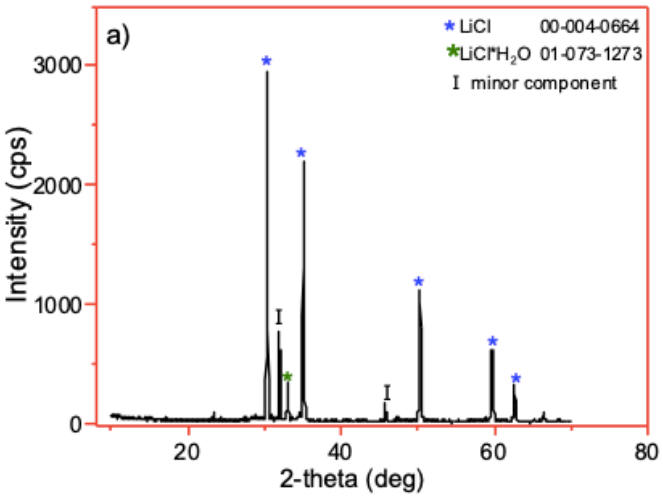

Preprints (www.preprints.org) | NOT PEER-REVIEWED | Posted: 25 October 2022 doi:10.20944/preprints202210.0372.v1

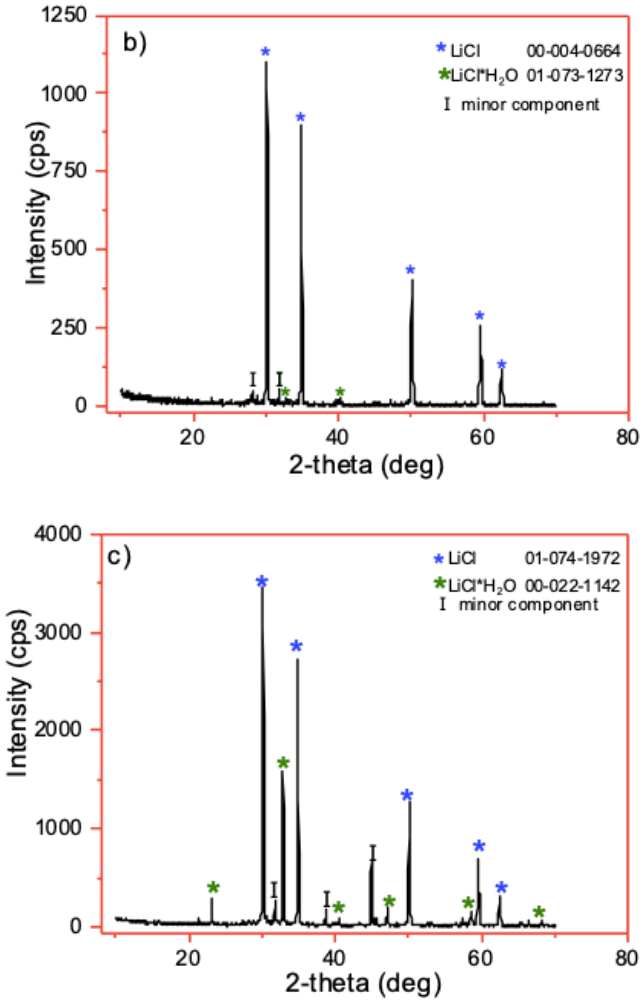

Figure 6. XRD patterns of the SP samples from the isothermal experiment at 700 °C for the BM/$CaCl_2$/CB system: a) VBM-1, b) VBM-2, and c) SBM.

Figure 7 presents the SEM micrographs of the SP samples. The particles of the three samples have a microscopic structure with a high degree of crystallization, agglomeration, and approximate laminated morphology with a smooth surface and a hexagonal shape. Elemental analysis shows the presence of Cl. These results confirm that LiCl is predominantly present in the SP samples. Therefore, lithium is extracted selectively as LiCl from each black mass sample by the process of carbochlorination with $CaCl_2$. Other elements are detected in SP samples by EDS; they are impurities that originated during sample preparation.

Preprints (www.preprints.org) | NOT PEER-REVIEWED | Posted: 25 October 2022 doi:10.20944/preprints202210.0372.v1

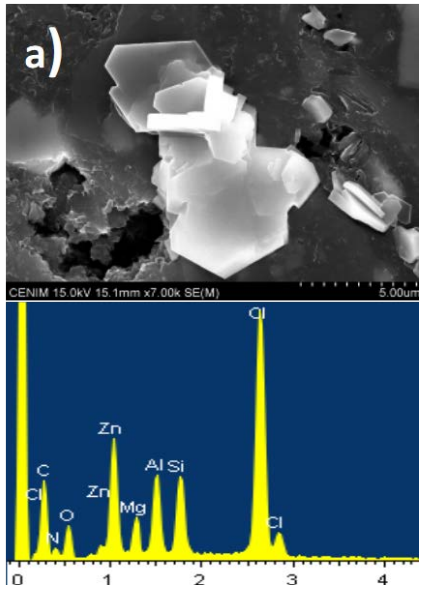

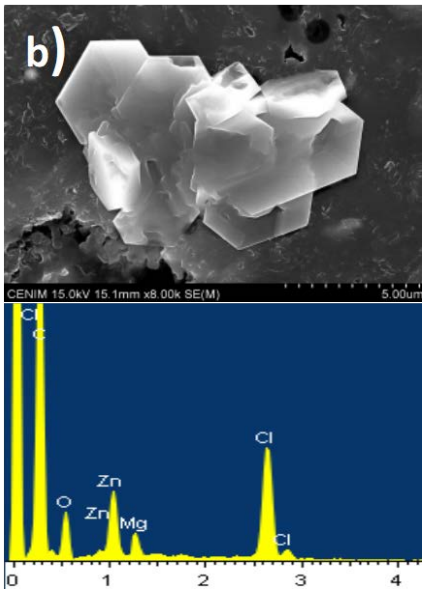

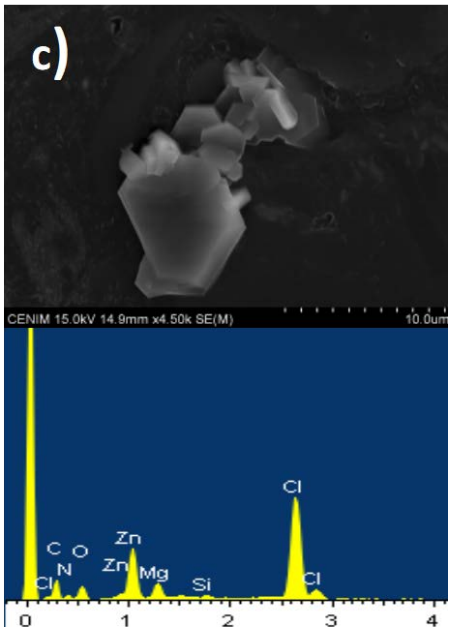

Preprints (www.preprints.org) | NOT PEER-REVIEWED | Posted: 25 October 2022 doi:10.20944/preprints202210.0372.v1

Figure 7. SEM micrographs and EDS spectra of the SP samples from the isothermal experiment at 700 °C for the BM/$CaCl_2$/CB system: a) VBM-1, b) VBM-2, and c) SBM.

Table 3 compares the lithium extraction results of both systems BM/$CaCl_2$ and BM/$CaCl_2$/CB from isothermal experiments performed at 500 and 700 °C. Lithium extraction values at 500 °C are higher than those obtained at 700 °C for both systems. A closer inspection of the table shows that extraction levels from the BM/$CaCl_2$/CB combination are considerably higher than those obtained from the BM/$CaCl_2$ combination. Quantitative extraction is reached from the BM/$CaCl_2$/CB combination at 700 °C for the three samples. Overall, extraction results agree with XRD results. With regards to XRD results of NSP samples, the levels of extraction agree well with either a significant decrease of the intensity peaks or complete disappearance of the original phase intensity peaks.

Table 3. Lithium extraction at 500ºC and 700ºC for 60 min.

Temperature (ºC)	BM/$CaCl_2$	X(%)	BM/$CaCl_2$/carbon black	X(%)
500	VBM-1	35	VBM-1	76
	VBM-2	35	VBM-2	80
	SBM	60	SBM	95
700	VBM-1	90	VBM-1	99
	VBM-2	90	VBM-2	99
	SBM	95	SBM	99

Together all the results indicate that the carbochlorination of the $LiMO_2$ structure (with M = Co, Ni-Mn, Ni) is feasible at 500 and 700 °C. The reaction leads to LiCl as the only chloride generated. The whole carbochlorination process can be represented by the following reaction equation (2):

$$4\,LiMO_2 + 2\,CaCl_2 + C \rightarrow 4\,LiCl + 2\,CaCO_3 + 4M + CO_2 \qquad (2)$$

Lithium is extracted from the structure of the initial $LiMO_2$ phase by the chlorinating action of calcium chloride. The presence of the carbon material favors the formation of $CaCO_3$. Also, the carbon material induces the reduction of any metal M to form metallic M. Temperature has a significant influence on lithium extraction and the products that can be evolved. Lithium extraction values at 700 °C are much higher than those at 500 °C for both systems BM/$CaCl_2$ and BM/$CaCl_2$/CB. In the case of VBM-1 carbochlorination, at 500 °C, the oxide $NiO_{0.7}5MnO_{0.25}$ is evolved, while the oxide $NiO_{0.7}5MnO_{0.25}$ and metallic Ni is evolved when the temperature is increased to 700 °C for the VBM-1/$CaCl_2$. At 500 °C, $NiO_{0.7}5MnO_{0.25}$ and MnO_2 are evolved, while MnO_2 and metallic Ni when the temperature is increased to 700 °C for the VBM-1/$CaCl_2$/CB system. In the case of VBM-2 carbochlorination, at 500 °C, no oxide is evolved, while NiO is evolved when the temperature is increased to 700 °C for the VBM-2/$CaCl_2$. At 500 °C, NiO is evolved, while NiO and metallic Ni are evolved when the temperature is increased to 700 °C for the VBM-2/$CaCl_2$/CB system. In the case of SBM carbochlorination, at 500 °C, CoO is evolved, while CoO and metallic Co are evolved when the temperature is increased to 700 °C for the SBM/$CaCl_2$/CB system.

The presence of carbon black also has a great influence on lithium extraction and reduction extent. Quantitative lithium extraction is achieved when carbon black takes part in the reaction system, while the maximum lithium extraction achieved is 95% when carbon black is not present in the system. The superior reduction action of carbon black is much notorious at 700 °C due to the presence of Ni and Co in their metallic state. However, the reduction from oxide to metal is not complete. Graphite, originally present in the black mass samples in high concentration, which in turn has a low reduction action as compared with carbon black [18,30] could be hindering the reduction reaction and preventing the complete reduction of Co and Ni to its elemental state. In addition, ash formed

 doi:10.20944/preprints202210.0372.v1

during the carbochlorination process may also be preventing the reaction of reduction of Co and Ni.

The present results are significant in at least two major respects. Lithium is selectively chlorinated using $CaCl_2$ as a chlorinating agent under the experimental conditions of the study. Then, LiCl can be easily recovered by water-leaching. Another interesting finding is that the addition of carbon black favors the yielding of Co and Ni in their metallic state. Thus, both metals can be separated magnetically from $CaCO_3$, another product of the carbochlorination reaction, and other impurities to fully recover the metals present in the black mass samples. Therefore, there is a need for further progress in determining the conditions and processes necessary to separate all metals from black mass samples with a high purity degree.

5. Conclusions

Carbochlorination using $CaCl_2$ as a chlorinating agent and elemental carbon as a reducing agent is an effective process to extract selectively lithium as lithium chloride from black mass samples with varied cathode chemistries from spent LIBs. Temperature and carbon form are the variables having the most marked effect on the carbochlorination process. The extraction of lithium increases with temperature and the use of carbon black as a reducing agent. Quantitative lithium extraction was achieved at 700 °C for 60 min in presence of carbon black in the reaction system. In addition, the process allows to recover Co, and Ni in their metallic state, which could be separated magnetically after a second calcination process. Finally, the researched methodology reveals that it is possible to effectively separate and recover different metals from discarded LIBs of different nature, leading to materials that could be used in the production of new batteries, which in turn could promote a circular economy and sustainable development goals.

Author Contributions: Conceptualization, F.A.L., L.B and J.G.; methodology, F.A.L. and J.G..; validation, Y.C.G., L.B. and L.A., formal analysis, Y.C.G., L.A. and F.J.A; investigation, Y.C.G. and L.A.; resources, F.A.L.; chemical analysis, F.J.A., writing—original draft preparation, Y.C.G..; writing—review and editing, L.A., L.B., J.G. and F.A.L.; supervision, F.A.L. and J.G..; funding acquisition, F.A.L. All authors have read and agreed to the published version of the manuscript.

Funding: This work has been funded by the European Union´s Horizon 2020 research under grant agreement No 776851 (Car-E Service).

Data Availability Statement: Not applicable.

Acknowledgments: Work carried out as part of the activities of the CSIC Interdisciplinary Thematic Platform PTI Mobility 2030 (https: //pti-mobility2030.csic.es/). The authors gratefully acknowledge the financial support of Consejo Nacional de Investigaciones Científicas y Técnicas CONICET (PUE 2017-071), Universidad Nacional de San Luis UNSL (PROICO 02-1420), Fondo para la Investigación Científica y Tecnológica FONCYT (PICT 2018-3878), and Fundación Carolina – SEGIB 2020-2021 for financing mobility for doctoral research. We acknowledge the support for the publication fee from the CSIC Open Access Publication Support Initiative through its Unit of Information Resources for Research (URICI).

Conflicts of Interest: The authors declare no conflict of interest.

References

1. Mirza, M.; Abdulaziz, R.; Maskell, W.C.; Tan, C.; Shearing, P.R.; Brett, D.J.L. Recovery of Cobalt from Lithium-ion Batteries using Fluidised Cathode Molten Salt Electrolysis. *Electrochim. Acta* **2021**, 138846, doi:10.1016/j.electacta.2021.138846.
2. Moazzam, P.; Boroumand, Y.; Rabiei, P.; Baghbaderani, S.S.; Mokarian, P.; Mohagheghian, F.; Mohammed, L.J.; Razmjou, A. Lithium bioleaching: An emerging approach for the recovery of Li from spent lithium ion batteries. *Chemosphere* **2021**, *277*, 130196, doi:10.1016/j.chemosphere.2021.130196.
3. Mossali, E.; Picone, N.; Gentilini, L.; Rodrìguez, O.; Pérez, J.M.; Colledani, M. Lithium-ion batteries towards circular economy:

A literature review of opportunities and issues of recycling treatments. *J. Environ. Manage.* **2020**, *264*, 110500, doi:https://doi.org/10.1016/j.jenvman.2020.110500.

4. Velázquez-Martínez, O.; Valio, J.; Santasalo-Aarnio, A.; Reuter, M.; Serna-Guerrero, R. A critical review of lithium-ion battery recycling processes from a circular economy perspective. *Batteries* **2019**, *5*, 5–7, doi:10.3390/batteries5040068.
5. Nasser, O.A.; Petranikova, M. Review of achieved purities after li-ion batteries hydrometallurgical treatment and impurities effects on the cathode performance. *Batteries* **2021**, *7*, doi:10.3390/batteries7030060.
6. Alcaraz, L.; Díaz-Guerra, C.; Calbet, J.; López, M.L.; López, F.A. Obtaining and Characterization of Highly Crystalline Recycled Graphites from Different Types of Spent Batteries. *Materials (Basel).* **2022**, *15*, 3246, doi:10.3390/ma15093246.
7. Chandran, V.; Ghosh, A.; Patil, C.K.; Mohanavel, V.; Priya, A.K.; Rahim, R.; Madavan, R.; Muthuraman, U.; Karthick, A. Comprehensive review on recycling of spent lithium-ion batteries. *Mater. Today Proc.* **2021**, doi:10.1016/j.matpr.2021.03.744.
8. Bankole, O.E.; Lei, L. Battery Recycling Technologies : Recycling Waste Lithium Ion Batteries with the Impact on the Environment In-View. **2017**, doi:10.5296/jee.v4i1.3257.
9. Magalini, F.; Kuehr, R.; Baldé, C.P. eWaste en América Latina. *GSMA Lat. Am.* **2015**, 1–38.
10. Romo, L.A.; López-Fernández, A.; García-Díaz, I.; Fernández, P.; Urbieta, A.; López, F.A. From spent alkaline batteries to $Zn_xMn_{3-x}O_4$ by a hydrometallurgical route: synthesis and characterization. *RSC Adv.* **2018**, *8*, 33496–33505, doi:10.1039/C8RA06789A.
11. Ji, Y.; Jafvert, C.T.; Zhao, F. Recovery of cathode materials from spent lithium-ion batteries using eutectic system of lithium compounds. *Resour. Conserv. Recycl.* **2021**, *170*, 105551, doi:10.1016/j.resconrec.2021.105551.
12. Barbosa, L.; Luna-Lama, F.; Peña, Y.G.; Caballero, A. Simple and Eco-Friendly Fabrication of Electrode Materials and Their Performance in High-Voltage Lithium-Ion Batteries. *ChemSusChem* **2020**, *13*, doi:10.1002/cssc.201902586.
13. Costa, C.M.; Barbosa, J.C.; Gonçalves, R.; Castro, H.; Campo, F.J. Del; Lanceros-Méndez, S. Recycling and environmental issues of lithium-ion batteries: Advances, challenges and opportunities. *Energy Storage Mater.* **2021**, *37*, 433–465, doi:10.1016/j.ensm.2021.02.032.
14. Zubi, G.; Dufo-lópez, R.; Carvalho, M.; Pasaoglu, G. The lithium-ion battery : State of the art and future perspectives. **2018**, *89*, 292–308, doi:10.1016/j.rser.2018.03.002.
15. Choubey, P.K.; Kim, M.S.; Srivastava, R.R.; Lee, J.C.; Lee, J.Y. Advance review on the exploitation of the prominent energy-storage element: Lithium. Part I: From mineral and brine resources. *Miner. Eng.* **2016**, *89*, 119–137, doi:10.1016/j.mineng.2016.01.010.
16. Olivetti, E.A.; Ceder, G.; Gaustad, G.G.; Fu, X. Lithium-Ion Battery Supply Chain Considerations: Analysis of Potential Bottlenecks in Critical Metals. *Joule* **2017**, *1*, 229–243, doi:10.1016/j.joule.2017.08.019.
17. Pagliaro, M.; Meneguzzo, F. Lithium battery reusing and recycling: A circular economy insight. *Heliyon* **2019**, *5*, e01866, doi:10.1016/j.heliyon.2019.e01866.
18. González, Y.C.; Barrios, O.C.; González, J.A.; Barbosa, L.I. Study on the carboreduction of the cathode material present in spent LIBs to produce Li_2CO_3 and CoO. *Miner. Eng.* **2022**, *184*, 107665, doi:10.1016/J.MINENG.2022.107665.
19. Zhou, L.F.; Yang, D.; Du, T.; Gong, H.; Luo, W. Bin The Current Process for the Recycling of Spent Lithium Ion Batteries. *Front. Chem.* **2020**, *8*, 1–7, doi:10.3389/fchem.2020.578044.
20. Yang, H.; Deng, B.; Jing, X.; Li, W.; Wang, D. Direct recovery of degraded $LiCoO_2$ cathode material from spent lithium-ion batteries: Efficient impurity removal toward practical applications. *Waste Manag.* **2021**, *129*, 85–94, doi:10.1016/j.wasman.2021.04.052.
21. Lei, S.; Zhang, Y.; Song, S.; Xu, R.; Sun, W.; Xu, S.; Yang, Y. Strengthening Valuable Metal Recovery from Spent Lithium-Ion Batteries by Environmentally Friendly Reductive Thermal Treatment and Electrochemical Leaching. *ACS Sustain. Chem. Eng.* **2021**, *9*, 7053–7062, doi:10.1021/acssuschemeng.1c00937.
22. Yue, Y.; Wei, S.; Yongjie, B.; Chenyang, Z.; Shaole, S.; Yuehua, H. Recovering Valuable Metals from Spent Lithium Ion Battery

via a Combination of Reduction Thermal Treatment and Facile Acid Leaching. *ACS Sustain. Chem. Eng.* **2018**, *6*, 10445–10453, doi:10.1021/acssuschemeng.8b01805.

23. Hu, J.; Zhang, J.; Li, H.; Chen, Y.; Wang, C. A promising approach for the recovery of high value-added metals from spent lithium-ion batteries. *J. Power Sources* **2017**, *351*, 192–199, doi:10.1016/j.jpowsour.2017.03.093.
24. Orosco, P.; Barbosa, L.; Ruiz, M.D.C. Synthesis of magnesium aluminate spinel by periclase and alumina chlorination. *Mater. Res. Bull.* **2014**, *59*, 337–340, doi:10.1016/j.materresbull.2014.07.026.
25. Barbosa, L.I.; González, J.A.; Ruiz, M.D.C. Extraction of lithium from β-spodumene using chlorination roasting with calcium chloride. *Thermochim. Acta* **2015**, *605*, 63–67, doi:10.1016/j.tca.2015.02.009.
26. Barrios, O.C.; González, Y.C.; Barbosa, L.I.; Orosco, P. Chlorination roasting of the cathode material contained in spent lithium-ion batteries to recover lithium, manganese, nickel and cobalt. *Miner. Eng.* **2022**, *176*, 107321, doi:10.1016/J.MINENG.2021.107321.
27. Movahedian, A.; Raygan, S.; Pourabdoli, M. The chlorination kinetics of zirconium dioxide mixed with carbon black. *Thermochim. Acta* **2011**, *512*, 93–97, doi:10.1016/j.tca.2010.09.006.
28. González, J.; Bohé, A.; Pasquevich, D.; Del, M. β-Ta_2O_5 carbochlorination with different types of carbon. *Can. Metall. Q.* **2002**, *41*, 29–40, doi:10.1179/cmq.2002.41.1.29.
29. González, J.A.; Rivarola, J.B.; Ruiz, M.D.C. Kinetics of chlorination of tantalum pentoxide in mixture with sucrose carbon by chlorine gas. *Metall. Mater. Trans. B Process Metall. Mater. Process. Sci.* **2004**, *35*, 439–448, doi:10.1007/s11663-004-0045-1.
30. González, J.; Ruiz, M.C. Del; Bohé, A.; Pasquevich, D. Oxidation of carbons in the presence of chlorine. *Carbon N. Y.* **1999**, *37*, 1979–1988, doi:10.1016/S0008-6223(99)00063-9.
31. 1997. Jena P.K., B.E.A. Mineral Processing and Extractive Metallurgy Review: An International Extractive Metallurgy of Beryllium. *Science (80-.).* **1997**, 37–41.
32. Tunez, F.M. Aparato de Laboratorio para realizar termogravimetrías en atmósferas corrosivas y no corrosivas 2007.
33. Zhao, B.L.; Li, N.; Langner, A.; Steinhart, M.; Tan, T.Y.; Pippel, E.; Hofmeister, H.; Tu, K.; Gösele, U. Crystallization of Amorphous SiO_2 Microtubes Catalyzed by Lithium. **2007**, 1952–1957, doi:10.1002/adfm.200601104.